General Disclaimer

One or more of the Following Statements may affect this Document

- This document has been reproduced from the best copy furnished by the organizational source. It is being released in the interest of making available as much information as possible.

- This document may contain data, which exceeds the sheet parameters. It was furnished in this condition by the organizational source and is the best copy available.

- This document may contain tone-on-tone or color graphs, charts and/or pictures, which have been reproduced in black and white.

- This document is paginated as submitted by the original source.

- Portions of this document are not fully legible due to the historical nature of some of the material. However, it is the best reproduction available from the original submission.

SOLIDIFICATION OF UNDERCOOLED LIQUIDS

J.H. Perepezko*, Y. Shiohara+, J.S. Paik* and M.C. Flemings+

*Department of Metallurgical and Mineral Engineering
University of Wisconsin-Madison
Madison, Wisconsin 53706

+Department of Materials Science and Engineering
Massachusetts Institute of Technology
Cambridge, Massachusetts 02139

ABSTRACT

During rapid solidification processing (RSP) the amount of liquid undercooling is an important factor in determining microstructural development by controlling phase selection during nucleation and morphological evolution during crystal growth. While undercooling is an inherent feature of many techniques of RSP, the deepest undercoolings and most controlled studies have been possible in carefully prepared fine droplet samples. From past work and recent advances in studies of nucleation kinetics it has become clear that the initiation of crystallization during RSP is governed usually by heterogeneous sites located at surfaces. With known nucleant sites, it has been possible to identify specific pathways of metastable phase formation and microstructural development in alloys. These advances have allowed for a clearer assessment of the interplay between undercooling, cooling rate and particle size statistics in structure formation. New approaches to the examination of growth processes have been developed to follow the thermal behavior and morphology in small samples in the period of rapid crystallization and recalescence. Based upon the new experimental information from these studies, useful models can be developed for the overall solidification process to include nucleation behavior, thermodynamic constraints, thermal history, growth kinetics, solute redistribution and resulting structures. From the refinement of knowledge concerning the underlying factors that govern RSP a basis is emerging for an effective alloy design and processing strategy.

Introduction

The main attention in rapid solidification (RSP) methods has been focused upon the attainment of high cooling rates in the range of 10^4 to 10^8 °C/sec. With these methods small liquid volumes are quenched either in contact with a substrate as in melt spinning and directed energy beam processing or in an inert gas as in atomization. However, the most important impact of RSP can be related directly to the solidification structures and the new opportunities for structure control by innovative alloy design and processing strategies. The wide range of reported microstructural variations encompass not only equilibrium phase mixtures with refined microstructural scale, but also novel microstructures such as supersaturated solid solutions, metastable intermediate phases and amorphous solids.

The existence and understanding of novel microstructures representing non-equilibrium phases requires a consideration of the level of undercooling at the onset of nucleation in addition to rapid growth kinetics. In fact, the available free energy for non-equilibrium phase formation is directly related to the amount of undercooling. With increasing levels of undercooling the product phase selection involved in nucleation can be expanded to involve an increased variety and to allow competitive growth kinetics to play an important role in the evolution of different microstructural morphologies. Accordingly, the examination of solidification in undercooled liquids can contribute to the basic understanding necessary for an effective microstructure control and alloy design in the optimization of RSP.

Experimental Techniques for High Undercooling

Even with liquid metals of high purity the attainment of a high level of undercooling is precluded usually by the catalytic action of residual impurities or container walls. In order to observe extensive undercooling it is necessary to circumvent the catalytic effects of the active nucleants. An effective experimental approach that may be applied to yield large undercooling prior to solidification involves the slow cooling (10-30°C/min) from the melt of a dispersion of stabilized fine metal

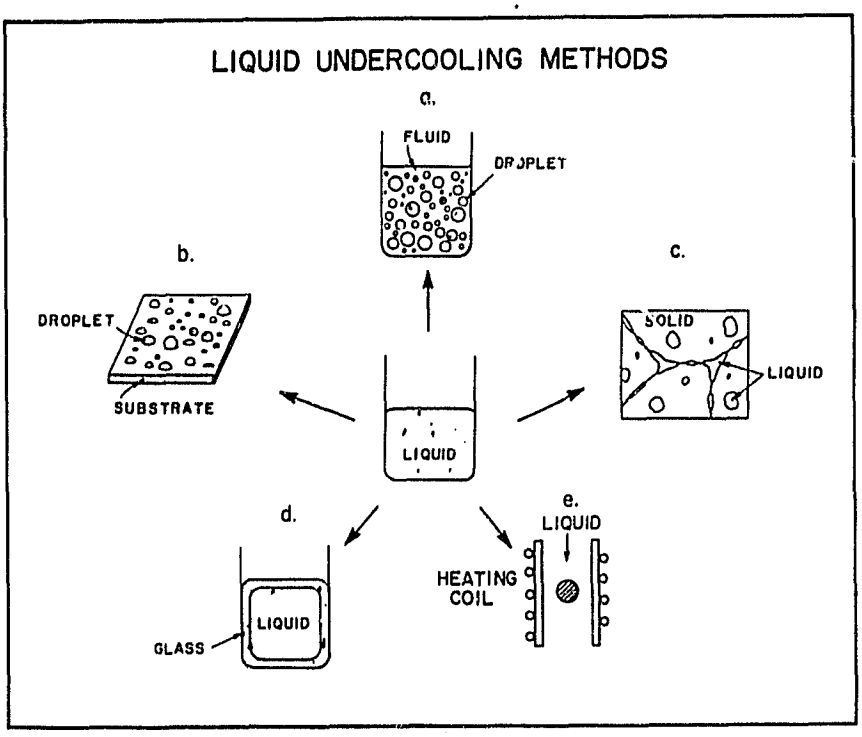

. Fig. 1 Liquid undercooling methods

droplets [1]. By starting with high purity metal and dispersing the liquid into a large number of small droplets (<20μ) within a suitable medium, the catalytic effects of active nucleants may be restricted to a small fraction of the total droplet population. A suitable means of carrying out the nucleant isolation operation is illustrated schematically in fig. 1.

In considering the droplet approach to undercooling, a distinction should be made between the several modifications of this technique which have been employed by a number of investigators in the past. For example in the droplet substrate method [2], a small sample of liquid metal is placed on an inert glass substrate in a chamber with an inert or reducing atmosphere. With this approach the onset of solidification is determined by visual observation of the change in surface reflectivity of a metal droplet which is about 50-100μ in diameter. In the entrained droplet technique [3] a bulk alloy sample is equilibrated in a liquid-solid two phase field with the temperature and alloy composition selected so that only a small fraction of the volume will be liquid in contact with a primary solid solution phase, as a potential heterogeneous nucleant. In addition, several other procedures have been developed for generating liquid metal droplet dispersions which exhibit a propensity for substantial undercooling. These droplet forming techniques involve exploding wires [4], shotting [5] and the containerless solidification in drop tubes [6]. While the majority of droplet undercooling schemes have a provision for some method of temperature measurement, the undercooling tendency of liquid droplets in several cases including all atomization methods is judged usually from microstructural observations.

With bulk samples, the removal of active nucleation sites usually involves a physical separation of the sites from the melt or a chemical treatment either to incorporate or to deactivate possible catalytic sites in the presence of an inorganic containment layer. These approaches which include a bulk sample encased in organic glasses [7] as well as a bulk melt levitated by induction [8] indicate that some remarkably large levels of undercooling (i.e. 0.2 T_m) may be achieved. The inorganic glass encasing is believed to promote undercooling not only by isolating the liquid from possible catalytic sites on container walls, but also by a possible scavenging action on nucleating centers that may be distributed within the volume of the melt. It is worthwhile to note that in principle the undercooling attained in properly conditioned bulk samples should approach the levels in droplet samples. Besides these specific undercooling techniques, it is clear that atomization of liquids is a commercial RSP method which incorporates an effective nucleant isolation operation as well as rapid quenching.

Nucleation Kinetics in Undercooled Liquids

In the present discussion the main interest in nucleation kinetics will be focused on the possible relationships between undercooling and cooling rate during the solidification of a distribution of liquid droplets. These relationships may be examined by nucleation rate calculations, but the computed results are highly dependent on the specific values assigned to the kinetic rate parameters. Reliable information is available for some parameters, however, in most cases the kinetic parameters are assigned values based upon theoretical models which require experimental verification. To minimize the uncertainty associated with calculations based model dependent parameter values, it is of interest to examine the range of droplet nucleation kinetics in a general manner. With this approach it is possible to deduce several useful guiding relationships for rapid solidification behavior.

Nucleation of a crystalline phase in an undercooled liquid phase may be classified into two mechanistic types. When nucleation occurs without an association with any catalytic nucleation sites, it can be classified as homogeneous nucleation. In the vast majority of experimental conditions nucleation is initiated at some catalytic nucleation site as heterogeneous nucleation. For a heterogeneous nucleation, an expression for the nucleation rate, J, has been developed on the basis of homogeneous nucleation theory [9] as:

$$J = \Omega_a \exp\left[-\Delta G(n^*)/kT\right] \tag{1}$$

where Ω_a is proportional to the number of liquid atoms in contact with unit area of the catalytic surface as well as the jumping frequency of atoms, $\Delta G(n^*)$ is the activation barrier for nucleation and kT has the usual meaning. For nuclei having the form of a spherical sector,

$$\Delta G(n^*) = (16/3)\,\pi\sigma^3\, f(\theta)/(\Delta G_v)^2 \tag{2}$$

where σ is the interfacial energy between the nucleus and the liquid, ΔG_v is the driving free energy for nucleation of unit volume of the product phase and $f(\theta) = (2-3\cos\theta + \cos^3\theta)/4$ is a contact angle factor. In the description of nucleation kinetics during rapid liquid quenching, steady state nucleation conditions may be considered in general, except for glass forming alloys [9].

Nucleation Rate Parameters

The nucleation rate is a relatively steep function of temperature with a steady state magnitude determined principally by the value of the exponential terms in $\Delta G(n^*)$ at the nucleation temperature T_n and to a lesser amount by the prefactor. In evaluating the temperature dependence of J usually a constant value based on theory is taken for Ω_a even though the catalytic site may vary. Similarly, little information is available to judge the catalytic potency, $f(\theta)$ so that a range of values is used in calculations. However, the most important parameters in determining J and hence the undercooling level are ΔG_v and σ which have received continued experimental and theoretical study.

In pure metals, the recent measurements of the heat capacity for undercooled liquids [10] have allowed for a direct evaluation of ΔG_v. In general, the experimental values are represented to within a few percent by the relation proposed by Turnbull [11,12].

$$\Delta G_v = -\Delta H_v\,(\Delta T/T_m) = -\,\Delta H_v\,(1-T_r) \tag{3}$$

where ΔH_v is the heat of fusion per unit volume of product phase, ΔT is the undercooling and T_m is the melting point of the product phase. For alloys the value of ΔG_v is determined from the composition of the nucleating phase at T_n. The composition dependence of ΔG_v can be expressed as

$$\Delta G_v = \left[X_A\,\Delta\mu^A + (1-X_A)\,\Delta\mu^B\right]/\bar{v} \tag{4}$$

where $\Delta\mu^A$ and $\Delta\mu^B$ are the chemical potential differences between the undercooled liquid and crystal and $\bar{v}$ is the molar volume for the crystalline phase at composition X_A. It is apparent from eq. 4 that ΔG_v is maximized when $\Delta\mu^A = \Delta\mu^B$ so that $\Delta G_v = \Delta\mu^A/\bar{v}$. This condition has been proposed by Hillert [13] to assess the nucleus composition. However, the favored nucleus composition should yield a minimum value of $\Delta G(n^*)$. Only if $\bar{v}$ and σ are not composition dependent can the maximum ΔG_v value occur at the same

composition as that for a minimum in $\Delta G(n^*)$. Apparently this behavior may be approached in some alloys. For example, recent calculations [14] of the composition dependence of the nucleation temperature, $T_n(x)$ have reproduced the observed experimental trends [1] which reflect the composition dependence of the liquidus, but the generality of the calculated behavior requires further examination.

In the study of nucleation one of the most important parameters is the solid-liquid interfacial energy. Since the nucleation rate is proportional to $\exp -(\sigma)^3$ as shown in eqs. 1 and 2, it is very sensitive to even slight errors in the σ value [15]. A direct measurement of σ is very difficult even with a large uncertainties because of sensitivity to impurity effects. Usually values of σ are calculated from classical nucleation theory by assuming that experimentally obtained maximum undercooling values are associated with homogeneous nucleation. Unless the maximum undercooling value is proven to refer to homogeneous nucleation, the estimated σ value is expected to underestimate the true value. There have been a number of theoretical approaches to study the structure and properties of the solid-liquid interface on the basis of various model constructions. The models range from the limiting cases in which σ values are calculated from enthalpic bond breaking arguments [16] or derived solely from a basis of entropic considerations [17] to intermediate approaches where a weighted contribution of enthalpic and entropic terms [18-20] is incorporated into the evaluation. At the present time, the theoretical values appear to underestimate σ compared to values calculated from nucleation undercooling results [15]. Certainly, an improvement in the independent experimental determination of σ would be invaluable in allowing for a clear evaluation of theoretical models and more reliable nucleation calculations.

Effect of Cooling Rate on Nucleation Kinetics

Since the onset of nucleation in a highly undercooled liquid is expected to be a sharp function of temperature it is useful to consider a limiting case for the effect of cooling rate on nucleation temperature. In general, for a given nucleation kinetics the critical condition to observe nucleation experimentally in a time, t, in a droplet of volume, v, and catalytic surface area, a, is given by $Jvt \simeq 1$ for homogeneous nucleation and by $Jat \simeq 1$ for heterogeneous nucleation. From eq. 1, the heterogeneous nucleation time can be represented as a function of temperature as:

$$\ln t = -\ln[a\ (\Omega_a)] + 16\ \pi\sigma^3 f(\theta)/[3\ k\ (\Delta H_v)^2\ T_m\ (1-T_r)^2\ T_r] \qquad (4)$$

where a Ω_a represents the heterogeneous nucleation site population associated with a droplet of volume v.

Furthermore, the rate dependence of the nucleation temperature which represents the shape of the T-T-T diagram associated with a specific nucleation kinetics is represented in general as

$$\frac{d\ T_r}{J(1nt)} = \frac{3k\ (\Delta H_v)^2\ T_m}{16\ \pi\sigma^3\ f(\theta)} \left[\frac{(1-T_r)^3\ T_r^2}{(3\ T_r - 1)}\right] \qquad (5)$$

where the possible temperature dependence of Ω_a, ΔH_v, σ and $f(\theta)$ has been neglected in order to examine a limiting value and minimize the uncertainty of model dependent values. For homogeneous nucleation $f(\theta) = 1$, but for a heterogeneous nucleation $0 \leq f(\theta) < 1$. Therefore, T-T-T diagrams for heterogeneous nucleation can have different breadths representing a different temperature dependence of the nucleation rate for different heterogeneous sites. In eq. 5, $dT_r/d(1nt)$ becomes infinite at $T_r = 1/3$ as the nucleation time is minimized. Therefore, $T_r = 1/3$ is believed to estimate a lower bound to the onset of sensible nucleation of a crystalline phase during slow cooling [21]. If the undercooling limit of the droplet sample represents the solidification of the nucleant-free droplet population, the crystallization temperature is determined either by the catalytic nature of the droplet surface coating or by the intervention of homogeneous nucleation kinetics. Also, during cooling the operation of a given catalyst kinetics and the kinetic competition between different catalysts and different product phase structures will be influenced strongly by the active catalyst distribution at the undercooling limit. In order to reach this limiting undercooling the size refinement of droplets becomes one of the most important factors. Further analysis on the distribution of active nucleants among droplets then becomes necessary to understand the undercooling behavior of droplet samples.

Nucleation Kinetics and Size Distribution Statistics

As long as a single nucleation kinetics with a steep temperature dependence is operating the effect of droplet size on the nucleation temperature is relatively small. In fact, if the size distribution is the only factor associated with the nucleation temperature range during cooling, a

sharp nucleation peak over a narrow temperature range (<10°C) is expected even with a sample of a rather broad droplet size distribution. However, droplet emulsion samples of pure metals and alloys often show a broad crystallization peak over a wide temperature range (>20°C). In this case the operation of a single nucleation kinetics is unlikely but the broad crystallization peak can be associated with multiple nucleation events continuously activated during the cooling process [21]. Morever, at a given cooling rate, nucleation of the crystalline phase in each droplet is associated with the catalytic potency of the most active nucleant. As a result, nucleation at different levels of undercooling due to crystallization over a wide temperature range can result in the formation of different structures in different droplets. Even if the same structure is nucleated at different levels of undercooling, this structure will not necessarily be retained completely in the final solidification pattern. For example, the final product structure can develop variations due to a different thermal history associated with the recalescence period following nucleation at different undercooling levels in separate droplets.

An example of the nucleation of different phases due to crystallization behavior over a broad undercooling range may be illustrated by considering the careful studies on Fe-Ni alloys reported by Cech [22]. In fine droplet samples, (<40μ), Cech demonstrated the presence of droplets of a metastable bcc structure in addition to droplets of the equilibrium fcc structure. Size distribution analysis results showed that small droplets less than 13μ are more likely nucleated at high undercooling since the major fraction had a metastable bcc structure. Since there were also droplets of the metastable structure within the large size grouping (d > 20μ), it is necessary to consider the mode of nucleant distribution among droplets. When all possible nucleation sites which can be activated a lower levels of undercooling than that necessary to retain the metastable phase are considered to be nucleants, a Poisson distribution function may be introduced to describe the random distribution of these nucleants among droplets [21,23]. In this case the fraction of droplets free from active nucleants is represented by

$$X = \exp [- m (v)] \qquad (6)$$

where m(v) is the average number of active nucleants in each droplet of volume V. Depending on the distribution mechanism of nucleants during the atomization process m(v) is proportional either to the volume or to the corresponding surface area of the droplet. Since a nucleant distribution proportional to the droplet volume would result in a rapid decrease in the yield of metastable product with increasing droplet size, it appears that for the Fe-Ni case, a surface area dependent nucleant distribution is most probable. A further application of the Poisson distribution has been reported for the solidification of Pd-Si droplet samples [24]. In this case the droplet fraction which solidified continuously as glass represents X in eq. 6 which can also be written in terms of droplet diameter, d, as $X = \exp [-(d/d_0)^n]$. When m(v) is proportional to the droplet surface area, n=2 for a heterogeneous surface nucleation. For heterogeneous volume nucleation n=3 and for homogeneous nucleation n=4.6. As in other droplet studies the solidification behavior of Pd-Si droplets was described most closely by a heterogeneous surface nucleation kinetics.

Metastable Phase Formation

Thermodynamic Features

A large number of examples of metastable phase formation have been demonstrated during rapid quenching experiments [25]. While the possible reaction paths leading to metastable phase formation in alloy systems are numerous a consideration of thermodynamic constraints can be useful in providing guidelines and limiting bounds on the reaction sequences in undercooled liquids. For example the free energy relationships that are relevant to the generation of solid solutions are illustrated in fig. 2. Two features are of interest in this case. For the formation of an equilibrium solid solution of composition C_0 at temperature T_N an overall free energy change of ΔG_1 is involved in reaction. However, in the early nucleation stage of reaction when a small amount of α forms from the liquid the driving free energy is maximized for α with a composition C_1 rather C_0. When the molar volume of solution does not change appreciably with composition, the C_1 composition may be determined by constructing a tangent to the α free energy curve which is parallel to a tangent to the liquid free energy. As noted previously, this consideration indicates that α with solute content different from C_0 can develop initially during nucleation [13]. Another feature of interest in fig. 2 concerns the bound set by the T_0 dashed curve between the liquidus and solidus [26], which represents the locus of equal free energy between liquid and solid. Formation of α product with the same composition as the liquid is excluded at compositions beyond the T_0 limit.

A thermodynamic consideration is of most value when the analysis also can provide an estimate of potential metastable intermediate phases that can enter in the kinetic competition. For example, in alloys the requirement that the free energy, ΔG, exhibit an overall decrease with reaction can lead to several interesting possibilities for phase reaction sequences [26] as illustrated by one example in

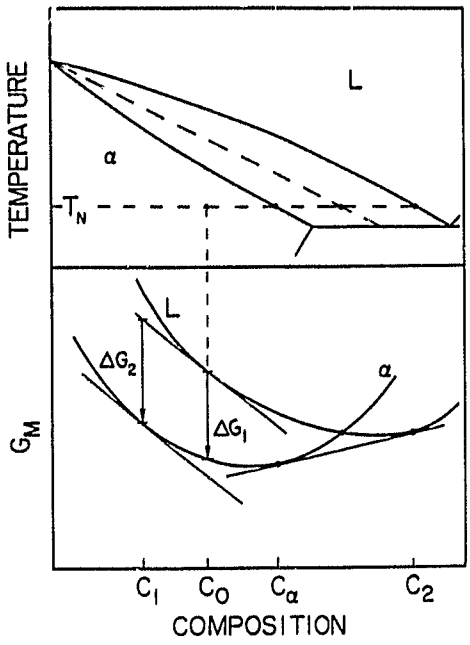

Fig. 2 Free energy relationship between undercooled liquid and α phase.

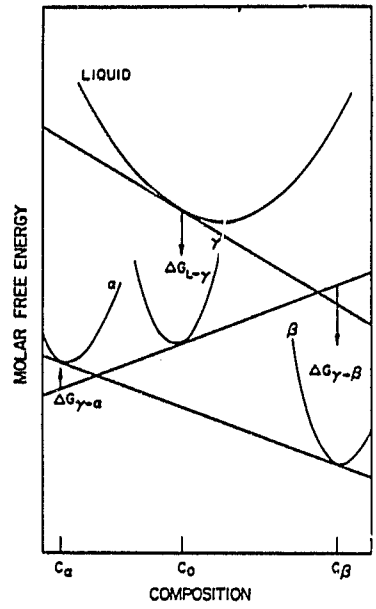

Fig. 3 Free energy relationship between undercooled liquid and several crystalline phases [26].

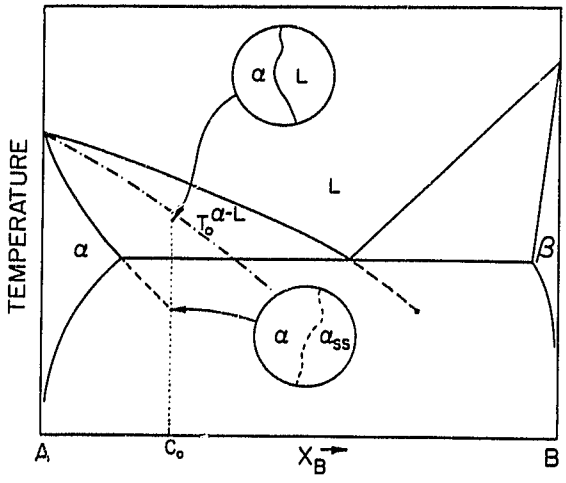

(a)

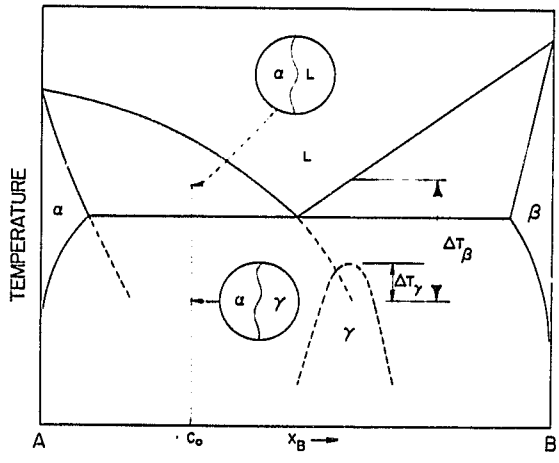

(b)

Fig. 4 Schematic illustration of a possible reaction path for primary phase catalysis of a metastable solid solution (a) and a metastable γ intermediate phase (b).

fig. 3. In this case the equilibrium solidification of liquid of composition C_0 would yield a two-phase mixture of α with composition C_α and β with composition C_β. However, if the nucleation kinetics are favorable, an intermediate reaction step can occur involving the formation of the metastable γ phase with composition C_0 and free energy reduction $\Delta G(L \rightarrow \gamma)$. The presence of γ phase affects the reaction sequence in that α phase cannot form since the free energy change $\Delta G(\gamma \rightarrow \alpha)$ is positive. Only after the γ phase transforms into β phase can the α phase form with a free energy reduction. When there are several metastable phases possible, the number of intermediate reaction steps can increase and present interesting opportunities for structure control during both solidification and subsequent solid state processing. One way of summarizing the potential for structure modification in alloys is to construct a metastable phase diagram [25,27].

Competitive Kinetics Analaysis

Since the driving force for the formation of a metastable phase is related directly to the amount of undercooling below the melting temperature of the phase, a high level of undercooling can expand the product selection involved in nucleation to an increased variety of types of structures. This is illustrated by the nucleation transition from fcc to bcc in Fe-Ni alloys [22], stainless steels [28] and tool steels [29]. Other examples have been reported in Pb-Bi, Bi-Cd and Pb-Sn alloys as well as Ga and Bi [1,10,21]. For Pb-Bi alloys a multiple phase selection transition has been observed in droplets [1]. As the level of undercooling increases an equilibrium eutectic mixture is replaced by a supersaturated (hcp) phase which in turn is superceded by a metastable intermediate phase at the highest undercooling. In addition for Pb-Sn, Sn-Ge and Cd-Sb alloys the operation of the nucleation product transition has been related to the catalytic effect of specific heterogeneous sites [21,30]. One type of effective nucleation site is a primary solid solution which can participate in catalysis reactions such as those illustrated in fig. 4 [21]. When the α phase is a potent catalyst, a continued growth of α is possible during cooling to form a supersaturated α product as in fig. 4a. When α is strongly catalytic in promoting the nucleation of a metastable intermediate γ phase as indicated in fig. 4b, the formation of an equilibrium β phase may be bypassed as the liquid is undercooled below the metastable γ phase melting point. Thus, for an alloy that may exhibit metastable products, it is possible to select a particular phase by controlling the degree of undercooling prior to solidification and by providing a high density of favorable catalytic sites.

In order to understand the kinetic competition between different phases during nucleation in an undercooled liquid, the comparison of thermodynamic stability may not be sufficient. In terms of overall nucleation kinetics, the driving free energy is not the only parameter of importance, but also nucleation site density and the magnitude of $\Delta G(n^*)$ associated with a given phase are critical. As an illustration of the application of nucleation kinetics to reveal the relationships between cooling rate, undercooling and phase selection, it is useful to consider the competition between two nucleation kinetics during continuous cooling of a droplet in several different situations that are illustrated in fig. 5. As an initial example, when two catalysts of different nucleation site density and potency are in the same droplet (B and C), the undercooling limit of the droplet at T_{r1} is determined by catalyst C at cooling rate $\dot{T}_1$. At cooling rate $\dot{T}_2$, however, the undercooling of the droplet increases to T_{r2} by circumventing the catalytic effect of C. Thus at a continually increasing level of cooling rate, there can be a significant improvement of undercooling as the catalytic effects of highly potent nucleants are circumvented. During this process the controlling nucleation kinetics involves catalysts of decreasing potency. When two different phases are competing with each other on the same catalytic surface present in a highly undercooled liquid, according to nucleation theory, the magnitude of the activation free energy barrier becomes the most dominant factor. Therefore, in order to favor nucleation of a metastable phase at a given cooling rate the activation energy barrier for the metastable phase should be lower than that for the equilibrium phase. In terms of eq. 1 this condition may be expressed as

$$\frac{\sigma_{LM}^{3} f(\theta')}{(\Delta H_v^m)^2 (1-T_r')^2} < \frac{\sigma^3 f(\theta)}{(\Delta H_v)^2 (1-T_r)^2} \qquad (7)$$

where σ_{LM} and θ' are the interfacial energy and the contact angle between the metastable phase and the catalytic surface, ΔH_v^m is the heat of fusion per unit volume of the metastable phase and T_r' is the relative nucleation temperature of the metastable phase. It has been shown in eq. 5 that the breadth of the T-T-T diagram associated with different nucleation kinetics is proportional to $(\Delta H_v)^2 T_m/\sigma^3 f(\theta)$ When the melting temperatures of two different phases nucleated by the same catalysts are very close and the metastable phase is dominant, the condition given by eq. 7 may be approximated by

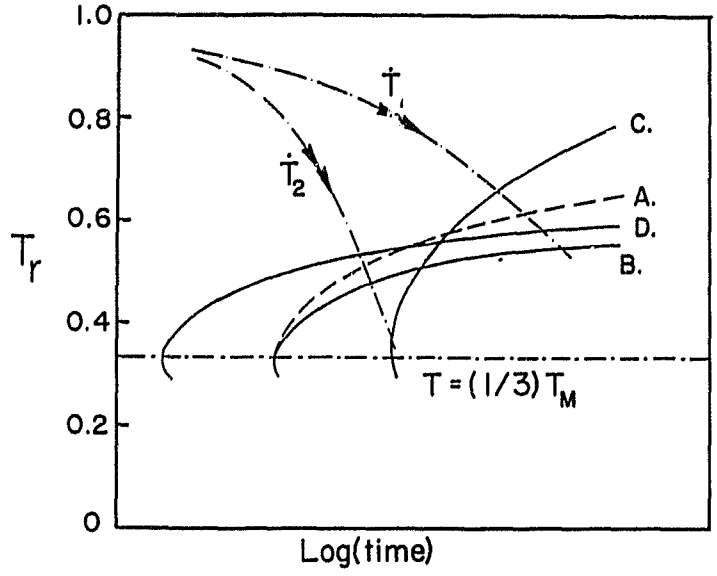

Fig. 5 T-T-T diagram representing different nucleation kinetics that may occur during a continuous cooling in undercooled droplets.

$$\frac{(\Delta H_v^m)^2}{\sigma_{LM}^3 f(\theta')} > \frac{(\Delta H_v)^2}{\sigma^3 f(\theta)} \qquad (8)$$

In this case, the breadth of the T-T-T diagram for the nucleation of the metastable phase (A) is larger than that for the equilibrium phase (B), but the noses of these two diagrams are placed at the same position as illustrated in fig. 5 schematically (A and B). Unless there are nucleants of higher catalytic potency for nucleation of the equilibrium phase (for example C in fig. 5), the equilibrium phase is always masked by nucleation of the metastable phase regardless of the cooling rate. In fact, the droplet emulsion technique which disperses potent nucleants of small population into a minor fraction of the droplet sample can be viewed as eliminating the possible activation of nucleation kinetics C in the major fraction of the sample. Alternatively, if the activation barrier for A is higher than that for B, the equilibrium phase will nucleate at all cooling rates. In addition, it is also possible for the nucleation of the equilibrium phase to be favored by an increase of the cooling rate if the nucleation site density for the equilibrium phase (curve D) is greater than that for the metastable phase. For these conditions an increase in cooling rate can result in a decreasing yield of a metastable product. In fact, a transition in nucleation from surface dependent to volume dependent kinetics with increasing cooling rate such as C to D in fig. 5 can yield a large increase in rate and may contribute to a propensity for multiple nucleation as reported in quenched Al-Si alloy droplets [31]. However, other factors involving the specific thermal history of droplets are also likely to contribute to the development of multiple nucleation.

In summary, the examination of the simple competitive kinetics examples reveals several types of general behavior. First, for a single operating kinetics an increase in cooling rate translates usually into some increase in undercooling. With several competing kinetics the increase in undercooling with cooling rate may not be uniform. For several competing kinetics and possible product structures, an increase in cooling rate can allow for nucleation of a metastable phase to be favored or for an increase in the yield of a metastable phase product, but this is not a general rule. Depending on the density of catalytic sites, it is possible for an increase in cooling rate to result in no change in phase selection or to result in a decreasing yield of a given metastable phase in favor of another metastable product or even an equilibrium phase product. From these examples illustrating the possible synergistic effects between high undercooling and rapid quenching to yield unique product structures, it is clear that attention to catalyst potency and site distribution as affected by surface conditions during atomization can be as important as cooling rate in optimizing RSP treatments.

Heat Flow and Pure Metal Solidification

In solidification of small droplets, two extreme heat flow situations may arise. In the first one, the solidification front moves into a liquid at its melting point or above, and the latent heat of fusion must be withdrawn through the solid. The second situation involves solidification into a supercooled melt. Nucleation occurs only after substantial supercooling, and initial solidification then occurs primarily by flow of heat into the liquid itself, therby resulting in droplet recalescence.

For solidification without undercooling, the Newtonian approximation is applicable when the dimensionless Biot number, Bi, is lower than 0.1, where $Bi = h\, r_o/k_m$. The Biot number is the ratio of the surface conductance or heat transfer coefficient, h to the metal conductance(k_m/r_o): k_m is the thermal conductivity of the metal and r_o is the droplet radius. The heat transfer coefficient is determined from the Nusselt number [32]:

$$Nu = 2\, h\, r_o/k_f - 2 + 0.6\, Re^{1/2} Pr^{1/3} \qquad (9)$$

where Re and Pr are Reynolds and Prandtl numbers respectively and k_f is the thermal conductivity of the fluid. In the case of solidification of metal droplets in a quiescent liquid or gas, the Nusselt number reduces to 2, and the Biot number is simplified to k_f/k_m. In the case of pure tin droplets emulsified in oil (polyphenylether), the Biot number is about 4.4×10^{-3}, since k_f is 0.112 kcal/m hr °C and k_m is 25.3 kcal/m hr °C. Thus, the dominant resistance to heat flow in this example occurs at the surface and no significant temperature gradients can develop inside the droplet in absence of undercooling. Similarly in most if not all gas atomization processes, heat transfer is limited by the solid-gas heat transfer resistance.

Thus, the simple Newtonian model is widely and correctly used for single phase cooling and solidification without undercooling [33]. Table 1 shows cooling rates for aluminum gas atomized droplets calculated in this way. Table 2 shows comparable cooling rates for atomized or emulsified metals in several liquid media.

When supercooling occurs in atomized or emulsified droplets, it is not obvious that the droplet will have a uniform temperature distribution during the recalescing period of solidification;

Table 1. Calculated Cooling Rates of Pure Aluminum at 660°C During Gas Atomization (in Helium at 300°K): (°K/sec)

Relative Gas Velocity		Particle Diameter(μm)	
mach	V_∞(m s^{-1})	10	100
0	0	7.21×10^6	7.21×10^5
0.1	97	1.00×10^7	1.56×10^6
0.3	290	1.22×10^7	2.26×10^6
0.5	483	1.36×10^7	2.69×10^6
1.0	965	1.56×10^7	3.53×10^6

Table 2. Calculated Cooling Rates of Pure Metal Droplets (10μm dia.) Cooled in Different Media at Low Reynolds Numbers

Metal and Quench Medium	Cooling Rate at Equilibrium Melting Point (°K/sec)
Aluminum in Helium gas at 27°C	7.21×10^6
Aluminum in Argon gas at 27°C	9.68×10^5
Aluminum in Liquid Gallium at 30°C	2.12×10^9
Tin in Argon at 27°C	4.57×10^5
Tin in Oil at 100°C	2.28×10^6
Tin in Oil/CCl_4(1/2) at -25°C	3.77×10^6
Iron in Argon at 27°C	1.15×10^6
Iron in Glass at 1000°C	3.99×10^7
Iron in Molten Salt at 482°C	3.11×10^6

i.e., the temperature of the growing interface may rise faster than the average temperature of the droplet. In this case, the validity of the Newtonian approximation during recalescence will depend not only on the Biot number, but also on interface velocity and interface morphology.

Levi and Mehrabian [34] have considered in some detail the solidification of undercooled droplets of pure metals, assuming a planar (non-dendritic) interface and the interface kinetic relationship suggested by Turnbull [35] and modified by Cahn [36] for the steady state continuous growth of a planar front. Figure 6 is an example of results of their computer calculations for an aluminum droplet with a single nucleation event. For the conditions chosen, significant temperature differences develop within the liquid during recalescence. Of course, as pointed out by Levi and Mehrabian, the magnitude and longevity of internal temperature differences depend sensitively on the number of nuclei growing, and on whether or not the interface is dendritic. In the case of multiple nucleation, the scale of the heat transfer problem is reduced from that of the droplet radius, r_0, to that of half of the interparticle spacing $d_{mx}/2$. In the limit of lacy dendrites (or, dendrites that become unstable and break into individual particles), the heat transfer scale is similarly reduced. Figure 7, also from Levi and Mehrabian, shows schematically how decreasing d_{mx} alters the "enthalpy path" during solidification. Decreasing d_{mx} moves paths more toward the top and right of the diagram and here recalescence becomes more rapid, more adiabatic, and more Newtonian.

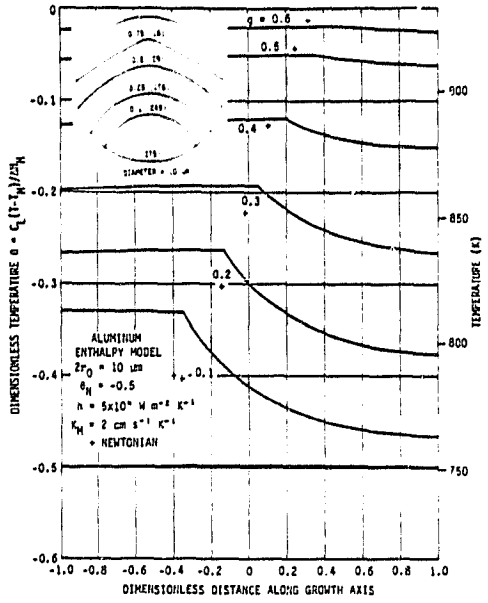

Figure 6. Thermal profiles for a recalescing pure aluminum droplet, 10μm dia. Advancing liquid solid front shown in insert which denotes fraction solid and interface velocity(cm s^{-1}), from Levi and Mehrabian [34].

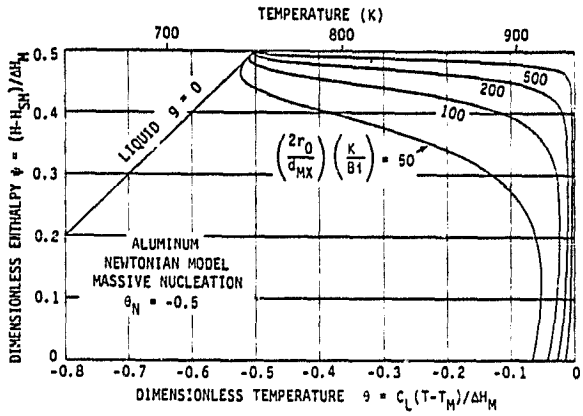

Figure 7. Effect of the ratio K/Bi on the thermal history of undercooled droplets for a fixed nucleation temperature. Note that for typical atomization conditions (k/Bi>100) the external cooling is not able to slow down recalescence to a significant extent, from Levi and Mehrabian [34].

We do not yet have experimental measurements of growth velocities or interface morphology in undercooled pure metal droplets. We can, however, turn to other studies where growth of crystals into pure undercooled liquids has been measured, and where this growth is apparently dendritic. Perhaps the highest measured crystal growth velocities are those of nickel and cobalt into their pure undercooled melts, reported by Walker [37], Colligan and Bayles [38]. In their experiments, columns of the bulk melt were undercooled by varying amounts up to 250-300°C and then seeded at one end. The velocity was determined from the times at which the freely moving dendrite tip passed thermal sensors sited along the column. Similar experiments have been performed by Glicksman et al [39] on succinonitrile, and successfully analyzed by combining heat flow and interface stability theory. By addition of interface kinetics to this analysis, Coriell and Turnbull [40] showed excellent agreement of theory with experiment, for the undercooled nickel experiments described above. These experimental studies, as well as interface stability theory suggest solidification of undercooled pure metals (and alloys) should be dendritic. Nonetheless, there are indications that undercooled alloy droplets at high undercooling solidify in a non-dendritic fashion. Perhaps this is because of transient effects, or perhaps because the wavwlength of the stability is long compared

with the droplet size [41].

Alloy Solidification

In an earlier section, the possibility has been described of achieving non-equilibrium phases through undercooling (e.g. obtaining a BCC phase in a normally austenitic steel). And of course, glassy structures can also be obtained. In this section, we focus on structure and segregation in alloys where the expected phases are formed (i.e. those obtained in usual solidification process).

A number of investigators have shown that solidification in bulk iron, nickel, and copper alloys is dendritic at moderate undercoolings, with the dendrite structure becoming gradually a simple rod-like structure with increasing undercooling. Then, at a critical undercooling which often seems to be about 100-200°C grain size drops abruptly; an example is shown in Figure 8 [42]. For undercoolings greater than the critical, the dendrite structure is completely absent, replaced by more-or-less spherical "elements" which are the separate grains [7,42]. Both the dendrite arm spacing in moderately undercooled specimens, and the size of the spherical elements are strongly dependent on cooling rate after recalescence. Hence, it is clear that the structures we see are strongly affected by ripening and are not therefore the actual structures that grew during recalescence. The abrupt grain size reduction has been althernately explained by an acoustic nucleation mechanism, and by a ripening or dendrite remelting mechanism.

Especially at intermediate to rapid rates of heat extraction during and/or immediately after recalescence, a number of investigators have observed solute rich cores within the dendrites or "elements" in undercooled alloys. Figure 9 is an example from work of Wu [43] showing high solute cores in 5mm dia. Fe-25%Ni alloy that was undercooled 90°C. The solute rich cores certainly formed during recalescence. Perhaps they grew in diffusionless fashion below the T_o, but the probable remelting, coarsening, and solid state diffusion occuring during and after recalescence did not completely eliminate these traces of the original structure.

Related structures have been obtained by Levi and Mehrabian in aluminum rapidly solidified droplets. Homogeneous solute rich material is found in a portion (or all) of the droplets when a given droplet is not completely homogeneous it contains also a solute depleted zone and dendritic or cellular region as well. The homogeneous solute rich region must have formed at some temperature below the thermodynamic T_o temperature, and grew in an apparently non-dendritic manner, at some critical temperature during recalescence, solute began to be rejected, eventually rendering it unstable and resulting in the cellular structure at the upper right.

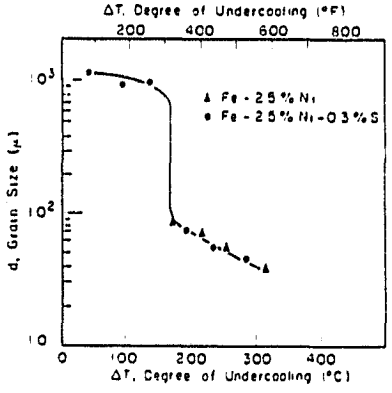

Figure 8. Grain size versus undercooling in a bulk undercooled melt, from Kattamis and Flemings [42].

Figure 9. Solute rich cores in undercooled Fe-25%Ni alloy, ΔT=90°C, 700X, from Wu [43].

With sufficient undercooling and sufficiently rapid heat extraction, supersaturated structures and non-equilibrium phases can be retained to room temperature. Kelly, Vander Sande and Cohen [28] have obtained a homogeneous (non-cellular), non equilibrium BCC structure in atomized 303 stainless steel powder in diameter up to about 70 microns. Figure 10 shows similar homogeneous structures in 316 stainless steel obtained by MacIsaac [44] in thesis work at MIT. These latter structures are of both the equilibrium FCC phase and the non-equilibrium BCC phase; they were obtained in an emulsification of steel in glass. These structures also appear to have grown in non-dendritic manner.

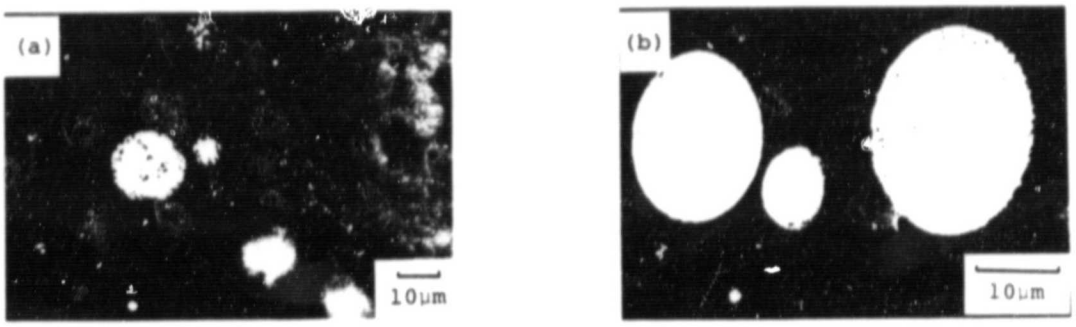

Figure 10. (a) Optical micrograph of cross-sectioned and etched 316 BCC and FCC particles after undercooling. Fcc particles are light in color. (b) Backscattered electron micrograph of the same particles, from MacIsaac [44].

The attributes of high undercooling and rapid heat extraction are optimized in emulsions when the emulsion itself is rapidly cooled by external means. One way to do this is shown in Figure 11 [45], where an emulsion of a metal in a carrier fluid is injected into a cooler miscible fluid that is being vigorously agitated. This is a technique developed by M.G. Chu in his doctoral thesis work at MIT. Figure 12 shows two structures of Sn-5%Pb alloy illustrating the importance of this external cooling. When the alloy is emulsified in such a way that it can achieve an undercooling of 100°C or more at slow cooling rates, and then is rapidly cooled using the apparatus of Figure 11, a fully homogeneous, non-dendritic structure is obtained, at least at 1000X, Figure 12a. This is in spite of the fact that the maximum equilibrium solid solubility of lead in tin is 2.5%. When, however, these samples are more slowly cooled, or reheated, or held for an extended period of time at room temperature, substantial precipitation of lead rich phase occurs, Figure 12b. In the case of Chu's work, the effect of the quench was probably primarily in preventing solid state decomposition. In other cases (e.g.) quenching liquid iron in molten salt. Table 2, heat extraction rates might conceivably be increased enough by the cold salt to influence solidification kinetics.

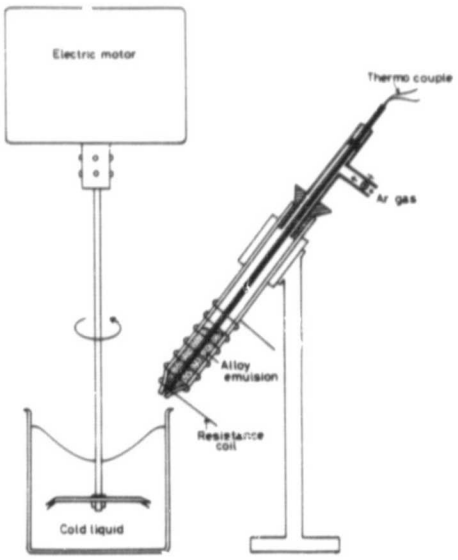

Figure 11. Diagram of apparatus for rapid quenching of molten emulsified droplets, from Chu et al [45].

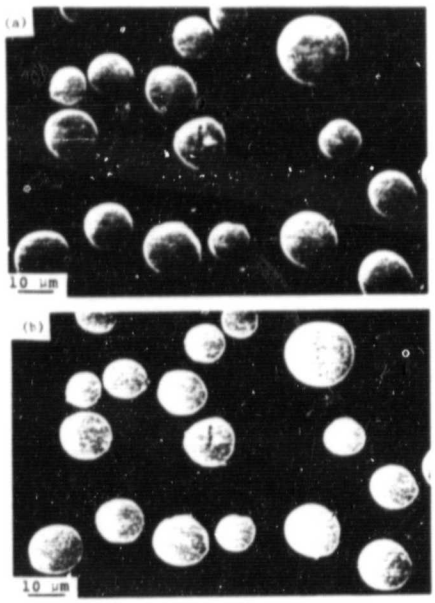

Figure 12. Microstructures of emulsified droplets of Sn-5%Pb: (a) Rapidly cooled to -25°C, (b) Rapidly cooled and then held one month at room temperature 1000X.

Quite complex solidification structures can be obtained in undercooled alloys when more than one phase forms during recalescence. Chu has studied a wide variety of such structures in tin-lead alloys; the structures obtained depend on alloy, undercooling and rate of heat extraction during and after recalescence. with the particular emulsification technique he used, and a moderate cooling rate (10°C/min), he found the nucleation temperatures plotted in the phase diagram in Figure 13a. A tin rich phase forms at T_n and a lead rich phase at T_n'. Perepezko [21] previously had found similar nucleation temperatures, Figure 13b, and by using a different emulsification medium, he was able to get the lower nucleation temperatures also shown in Figure 13b.

Solidification of hyper-eutectic tin-lead alloys was found to occur in the following sequence: (a) nucleation at T_n' of a lead rich phase, (b) dendritic growth of this phase, first during recalescence and then during subsequent cooling T_n, where a tin rich phase nucleates, (c) growth of the tin rich phase during recalescence and during subsequent cooling. Note that the recalescence and solute distribution during growth of the second phase can be expected to influence the first phase to form. In addition the intervention of the formation of a metastable phase prior to the tin rich phase due to catalysis by the lead rich phase [16] can also influence the overall solidification sequence and microstructure. Figure 14 shows examples of solidification structures of such an alloy. Figure 14a is a strucutre that was undercooled and rapidly quenched. Lead rich dendrites (white) first formed and tin rich phase (dark) later filled in within the interstices. Both the tin rich and lead rich phases shown substantial second phase with themselves, presumably from solid state precipitation. Figure 14b is a sample that was allowed to nucleate on slow cooling and then rapidly solidified. The dendritic structure formed as before, and the final structure is very little different. The sample allowed to cool slowly (10°C/min) however, shows massive ripening of the original lead rich phase, Figure 14c.

Three different tin-lead structures of eutectic composition are shown in Figure 15. The first is comparable to the slowly cooled Sn-45%Pb alloy discussed above, in that it shows primary, ripened lead rich phase (with entrapped and precipitated tin rich phase), Figure 15a. The second shows the same alloy rapidly cooled, Figure 15b. Apparently the rapid cooling suppressed the nucleation temperature of the lead rich phase, T_n' below that of the tin rich phase, T_n. The third structure, Figure 15c, from work of Cooper, Anderson and Perepezko [46] is similar to 15b, but somewhat coarser. In this case the nucleation temperature T_n' was depressed below T_n by a modified emulsion; this depression is shown in figure 13. The second two eutectic structures are similar to those obtained in conventional rapid solidification processes, e.g. wheel casting [47].

Recalescence Measurements in Droplet Solidification

Ewing [48] and Wu [43] in separate theses at MIT are attempting to gain some experimental understanding of the "solidification paths" of undercooled alloys by looking at thermal behavior and structure of 5mm dia. metal droplets undercooled in molten glass. Their results to date illustrate well how much we do not understand yet about this process.

As one example, the rate of recalescence of the droplet surface increases dramatically with increasing undercooling, Figiure 16. We believe that this cannot be a heat flow caused phenomenon since experiments on pure nickel show orders of magnitude faster recalescence. Thus, a preliminary conclusion is that these rates of recalescence (at least at temperatures approaching and above the calculated T_0) are limited by solute transport. The T_0 temperature in Figure 16, incidentally, was calculated from a regular solution model.

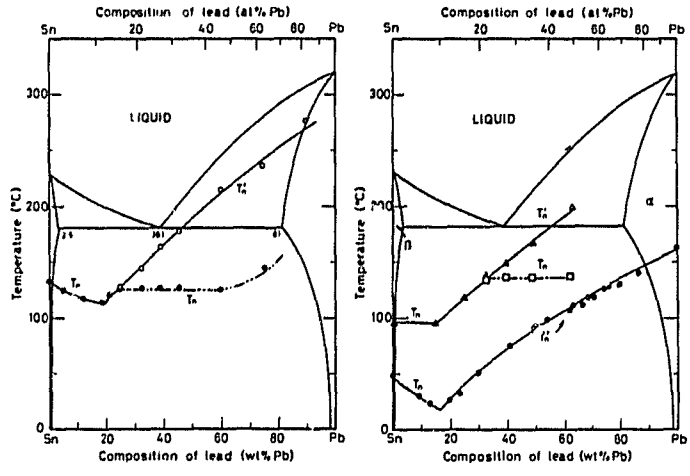

Figure 13. Nucleation temperature in supercooled Sn-Pb alloys. T_n is nucleation temperature of tin rich phase and T_n' of lead rich phase. Diagram on left is from Chu et al [45] and on the right is from Cooper et al [46]. Exact amounts of undercooling depend on emulsification procedure. The two different sets of curves in diagram on the right result from the different emulsification procedures.

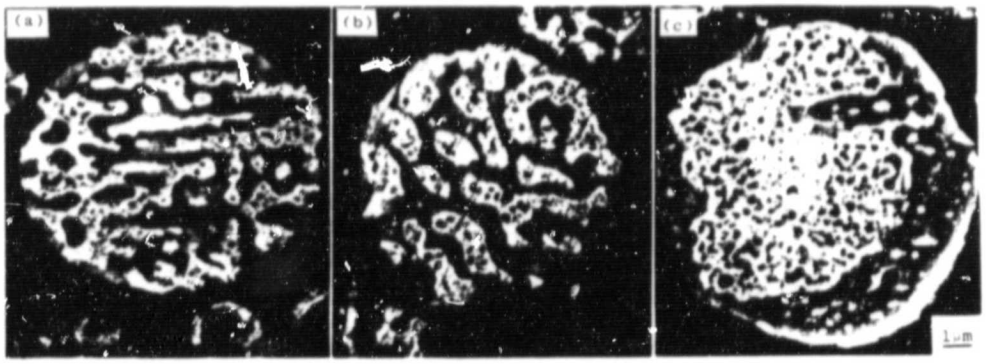

Figure 14. Microstructures of Sn-45%Pb alloy droplets, 7000X. (a) Rapidly quenched (b) Slowly cooled to just below T_n and quenched (c) Slowly cooled to room temperature.

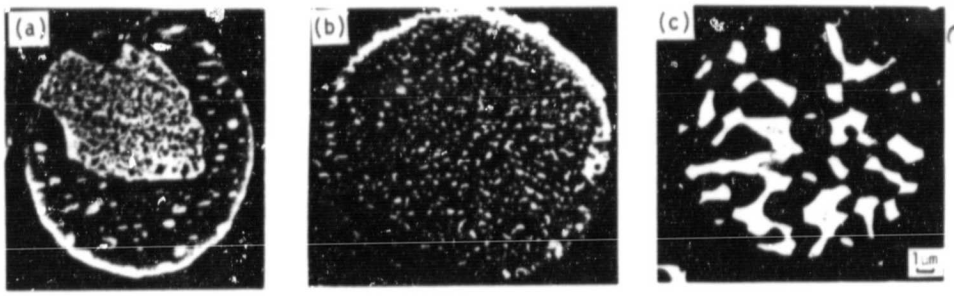

Figure 15. Microstructures of emulsified droplets of eutectic Sn-Pb alloy. (a) Slowly cooled, moderate undercooling, (b) Undercooled and rapidly solidified, (c) Slowly cooled, high undercooling.

The photomicrographs in Figure 17 provide some insight into factors influencing this recalescence, by showing the very different structures at different undercoolings. At moderate undercooling where temperature is estimated to be above the thermodynamic T_0 temperature, recalescence is very slow, and a two phase structure results that has a coarse dendritic appearance, Figure 17a. Initial results show the core of this "dendrite" is of approximately C_0 composition, the periphery is depleted, and the interdendritic regions appear to be somewhat above C_0, possibly it grew as a single phase initially into solute redistribution at least during later stages of growth. If so, we would expect re-melting on a fine scale within the dendrites as it recalesces above some temperature approaching T_0; the liquid pools remelting could lead to the finely distributed second phase within the "dendrite".

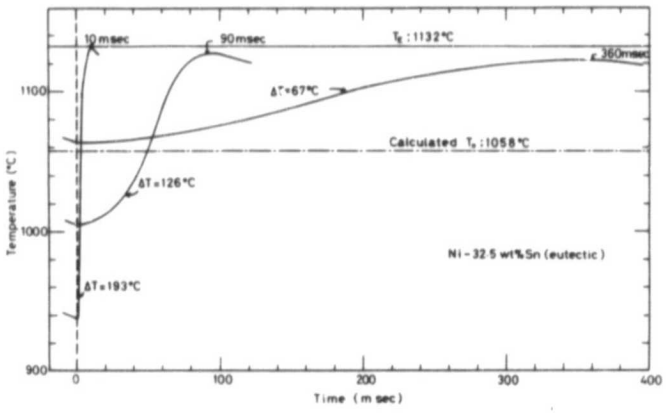

Figure 16. Recalescence curves from 5mm droplets of Ni-Sn eutectic alloy at several undercoolings, from Ewasko [48].

The sample at the intermediate undercooling in Figure 17 show a fine grain structure with a multiplicity of growth sites, each of which has a central region (two phase) that may well have

initially grown in a diffusionless manner below T_0 and later partially remelted during recalescence. The fine scale of this structure due to the multiplicity of growth sites would explain the more rapid recalescence, even above T_0. This qualitative description of solidification behavior for such an alloy is largely conjecture, but the approach suggests an experimental direction toward an eventual fuller thermal and solidification description of undercooled alloys.

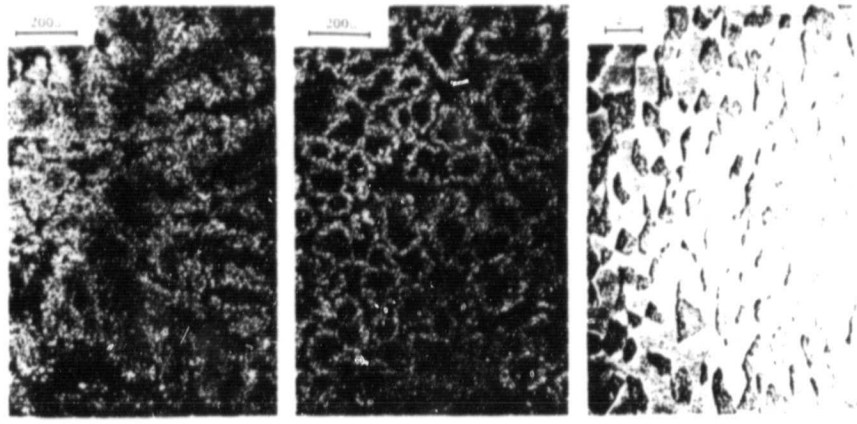

Undercooling 70°C Undercooling 120°C Undercooling 380°C

Figure 17. Structure of 5mm droplets of Ni-Sn eutectic alloy solidifed at 3 different undercoolings, from Wu [43].

Conclusions

In examining the nucleation and solidification of undercooled liquid metals it is apparent that the experimental and theoretical understanding has made good progress since the initial pioneering work of Turnbull. From the present experience with droplets studies it has been possible to identify some general guidelines for the interplay between process variables such as cooling rate, undercooling, alloy composition and particle size and the nucleation phase selection involved in RSP. With droplet samples and controlled undercooling conditions new understanding has been gained into the development of solidification microstructure and the influence of thermal history on the final microstructural morphology. This area of research in the study of RSP, we believe, has a great potential for the further development of nucleation and solidification theory. It also has the potential for the development of new processes of engineering importance. In this regard it seems possible that we can someday learn to enhance undercooling with controlled surface treatments in existing RSP methods, and perhaps, as well, find ways to bring other processes such as emulsification to the point of engineering usefulness.

Acknowledgement

The support and the ARO (DAAG29-80-K-0068) for studies on solidification structures and the NSF (DMR-79-15802) for work on nucleation catalysis kinetics at the University of Wisconsin-Madison is gratefully acknowledged. Portions of this work (those at MIT) were sponsored by NASA Grant No. NSG 7645, from Materials Processing & Space Division, NASA office, with Dr. Louis Testardi, project monitor.

References

[1]. J. H. Perepezko, in Proceedings of Rapid Solidification Processing: Principles and Technologies II, R. Mehrabian, B. H. Kear and M. Cohen eds., Claitor's Pub., Baton Rouge, La. 56 (1980).

[2]. D. Turnbull and R. E. Cech, J. Appl. Phys. 21, 804 (1950).

[3]. C. C. Wang and C. S. Smith, Trans. AIME 188, 136 (1950).

[4]. E. Meyer and L. Rinderer, J. Crystal Growth, 28, 199 (1975).

[5]. R. E. Cech and D. Turnbull, Trans, AIME, 206, 124 (1956).

[6]. L. L. Lacy, M. B. Robinson and T. J. Rathz, J. Crystal Growth 51, 47 (1980).

[7]. T. Z. Kattamis and M. C. Flemings, Trans. AIME 236, 1523 (1966).

[8]. S. Y. Shirashi and R. G. Ward, Canadian Met. Quaterly, 3, 117 (1964).

[9]. D. Turnbull, J. Chem. Phys., 20, 411 (1952).

[10]. J. H. Perepezko and J. S. Paik, in Proceedings of the 29th Midwest Solid State Conference: Novel Materials and Techniques in Condensed Matter, G. Crabtree and P. Vashishta eds., North Holland, N.Y., 57 (1982).

[11]. D. Turnbull, J. Chem. Phys., 18, 198 (1951).

[12]. C. V. Thompson and F. Spaepen, Acta. Met., 27, 1855 (1979).

[13]. M. Hillert, Acta Met., 1, 763 (1953).

[14]. C. V. Thomson and F. Spaepan, in Proceedings of the Materials Research Society Symposium: Materials Processing in the Reduced Gravity Environment of Space, G. E. Rindone eds., North Holland, N.Y., 603 (1982).

[15]. J. S. Paik and J. H. Perepezko, to be published.

[16]. A. S. Skapski, Acta Met., 4, 576 (1956).

[17]. F. Spaepen and R. B. Meyer, Scripta Met., 10, 257 (1976).

[18]. R. H. Ewing, Phil. Mag., 25, 778, 1972.

[19]. A. Bonnissent, J. L. Finney and B. Mutaftschiev, Phil. Mag. B, 42, 2, 233 (1980).

[20]. Y. Waseda and W. A. Miller, Trans. JIM, 19, 547 (1978).

[21]. J. H. Perepezko and J. S. Paik, in Proceedings of the Material Research Society Symposium: Rapidly Solidified Amorphous and Crystalline Alloys, B. H. Kear, B. C. Giessen and M. Cohen eds., North Holland, N.Y., 49 (1982).

[22]. R. E. Cech, J. Metals, 8, 565 (1956).

[23]. D. Turnbull, Acta Met., 1, 8 (1953).

[24]. A. J. Drehman and D. Turnbull, Scripta Met., 15, 543 (1981).

[25]. B. C. Giessen and R. H. Willens in Phase Diagrams: Materials Science and Technology Vol. III, A. M. Alper ed., Academic Press, N.Y., 104 (1970).

[26]. J. C. Baker and J. W. Cahn, in Solidification, ASM, Metals Park, Ohio, 23 (1971).

[27]. J. L. Murray, to be published

[28]. T. F. Kelly, M. Cohen and J. B. Vander Sande, submitted to Metal Trans. A,(1982).

[29]. C. M. Adam, Private Communication.

[30]. I. E. Anderson, J. H. Perepezko and B. C. Giessen, to be published.

[31]. C. G. Levi and R. Mehrabian, Met. Trans. 13A 13 , [illegible] (1982).

[32]. G.H. Geiger and D.R. Poirier: "TRANSPORT PHENOMENA IN METALLURGY", Addison-Wesley Publishing Company, Reading, MA(1973).

[33] N.J. Grant, in "RAPID SOLIDIFICATION PROCESSING-PRINCIPLES AND TECHNOLOGIES I", Baton Rouge, Claitor Publishing Division, 230(1978).

[34] C.G. Levi and R. Mehrabian, "HEAT FLOW DURING SOLIDIFICATION OF UNDERCOOLED METAL DROPLETS", ~~to be published.~~ Met. Trans. 13A 221 (1982)

[35] D. Turnbull, "THERMODYNAMICS IN PHYSICAL METALLURGY", Americal Society for Metals, Metals Park, OH(1949).

[36] J.W. Cahn, W.B. Hilling and G.W. Sears, Acta. Met., 12, 1421(1964).

[37] J.L. Walker, unpublished work presented in "PRINCIPLES OF SOLIDIFICATION", B. Chalmers, Chapter 4, John Wiley(1964).

[38] G.A. Colligan and B.J. Bayles, Acta. Met., 10, 895(1962).

[39] M. E. Glicksman, R.J. Schaefer, and J.D. Hyers, Metall. Trans. 74, 1947(1976).

[40] S.R. Coriell and D. Turnbull, submitted Acta. Met.(1981).

[41] W.J. Boettenger, S.C. Coriell, R.E. Sekerka, RAPID SOLIDIFICATION PROCESSING PRINCIPLES AND TECHNOLOGIES III., to be published.

[42] T.Z. Kattamis and M.C. Flemings, Trans. A.F.S., 75, 191(1967).

[43] Yan-Zhong Wu, unpublished work, Massachusetts Institute of Technology.

[44] D.G. MacIsaac, Y. Shiohara, M.G. Chu and M.C. Flemings submitted Proc. AIME Fall Meeting (St. Louis 1982).

[45] M.G. Chu, Y. Shiohara, M.C. Flemings, submitted Proc. AIME Fall Meeting (St. Louis 1982).

[46] K.P. Cooper, I.E. Anderson and J.H. Perepezko, Proc. 4th Int. Conf. on "RAPIDLY QUENCHED METALS VOL. 1" 107, Sendai, Japan(1981).

[47] R. Cheese and B. Cantor, Materials Science and Engineering, 45, 83(1980).

[48] Ricky Ewasko, S.M. Thesis, Department of Materials Science and Engineering, Massachusetts Institute of Technology(1982).